Applied Thermal Engineering 30 (2010) 2109–2115

Contents lists available at ScienceDirect

Applied Thermal Engineering

journal homepage: www.elsevier.com/locate/apthermeng

Analysis of thermal response of a food self-heating system

Son H. Ho [a,b], Muhammad M. Rahman [b,*], Aydin K. Sunol [c]

[a] Department of Mechanical, Materials and Aerospace Engineering, University of Central Florida, 4000 Central Florida Blvd., ENGR 307, Orlando, FL 32816, USA
[b] Department of Mechanical Engineering, University of South Florida, 4202 E. Fowler Avenue, ENB 118, Tampa, FL 33620, USA
[c] Department of Chemical and Biomedical Engineering, University of South Florida, 4202 E Fowler Avenue, ENB 118, Tampa, FL 33620, USA

ARTICLE INFO

Article history:
Received 10 March 2010
Accepted 18 May 2010
Available online 27 May 2010

Keywords:
Unitized Group Ration-Express (UGR-E)
Flameless Ration Heater (FRH)
Composite medium heat conduction
Exothermic reaction
Reactive magnesium heater
Chemical self-heating

ABSTRACT

This paper presents a distributed model of heat transfer in a self-heating unit for group meals and its numerical simulation. A magnesium alloy and water exothermic reaction provides the necessary energy. The resulting governing equations of chemical reaction and heat conduction that depicts the heater performance were solved to develop an approximate analytical solution, to which experimental data found from literature were compared and curve fitted. Then, a model of a complete food-heating unit for group meals, which include a stack of four sets of food tray, heating tray, and heater sandwiched between them, as well as the cardboard container, was developed. The governing equations for heat conduction in the complete model were solved. The response in thermal performance of the heating system to the parameters that influence heating profiles of the heater such as decay constant and heat generation capacity were studied. The results show that the system thermal performance is most significantly affected by heat generation and a proper combination of heaters with different heat generation capacity can improve temperature uniformity between food trays. The results are useful for designing and optimizing self-heating multi-food tray units.

1. Introduction

Self-heating food technology has been developed for more than a half of a century. Caldwell and Gillies [1] in 1950 described investigations leading to satisfactory reaction mixture for heating food compositions incorporated in can which could be charged with soups or other liquid foods and several millions of these cans were used during war. In the UK, it was reported in 1960 [2] that self-heating can originally developed as wartime expedient was made available to general public for use wherever other forms of heating were not suitable. Products include three soups and two beverages available to rally drivers, campers, picnickers, etc. Presently, there are many self-heating products that are commercially and widely available, including both food and drink. Oliver-Hoyo et al. [3] presented a classroom activity where a self-heating beverage and the Meals, Ready to Eat (MRE) were used as a real-life chemistry problem. Most of the developments of self-heating food products are presented in the form of patents. Kolb [4] described an insertable thematic module for self-heating cans. This heater contains a liquid reactant and a solid reactant, which is calcium oxide combined with a wax-based inhibitor. Pickard et al. [5] presented a self-heating group meal assembly that can hold a number of food pouches and used exothermic chemical heaters that contained Mg–Fe alloy. Lamensdorf [6] proposed a heater using powder mixture of Mg–Fe alloy that improved its performance as demonstrated by included experimental data.

The Unitized Group Ration-Express™ (UGR-E™) module is a compact, self-heating unit that provides a complete, hot meal for up to 18 soldiers in remote locations [7,8]. It has been approved by all departments of the Department of Defense [7] and available for procurement since 2007 [9]. UGR-E was developed by the Army based on the Flameless Ration Heater (FRH) technology [10] to heat the food. Detail specifications of the heaters and the food-heating system are described in [11]. A collection of military specifications related to UGR-E is available at [12]. UGR-E heating unit consists of a stack of four tray sets, put in a corrugated cardboard container box. Each tray set includes a heating tray, made of high-density polyethylene (HDPE) that houses a polymeric food tray and an activation fluid pouch at its bottom. All four activation fluid pouches of the four tray sets are connected to the activator tab. The main component of the UGR-E heating system is the heater, which contains a magnesium–iron compound that can be activated by a saline solution to initiate an exothermic chemical reaction. When food heating is required, four heaters (previously packed separately) are to slip beneath the food trays into the spaces between each pair of heating tray and food tray. Then the cover of the

* Corresponding author. Tel.: +1 813 974 5625; fax: +1 813 974 3539.
E-mail address: mmrahman@usf.edu (M.M. Rahman).

1359-4311/$ – see front matter © 2010 Elsevier Ltd. All rights reserved.
doi:10.1016/j.applthermaleng.2010.05.020

Nomenclature

c_p	Specific heat, J/kg K
m	Mass, kg
k	Thermal conductivity, W/m K
G	Heat generation, J
h	Heat transfer coefficient, W/m^2 K
k	Thermal conductivity, W/m K
n	Unit normal vector on a boundary
Q	Heat generation rate, W
q	Heat generation rate per unit volume, W/m^3
t	Time, s
T	Temperature, °C
V	Volume, m^3

Greek symbols

ΔH_{rxn}	Enthalpy change of reaction, J/kg
ΔT	Temperature rise, °C
δ	Thickness, m
λ	Reaction rate constant or decay constant of heating profiles, s^{-1}
ρ	Density, kg/m^3

Subscripts

0	Maximum
a	Air
amb	Ambient
b	Base case
c	Cardboard
f	Food
h	Heater
init	Initial
l	Lid
pe	Polyethylene (heating tray material)
pp	Polypropylene (food tray material)
r	Reactive magnesium
w	Water (in test pouch)

Superscripts

*	Dimensionless

container box is closed. As the activation tab is pulled, activation fluid floods the bottom of the trays and activates all the heaters simultaneously. Once the heaters are activated, the chemical reaction generates heat to get the meals ready in up to 45 min.

Most of the study and development in the field of food self-heating employed the experimental approach, which is practical and suitable for fast design to market applications. However, numerical modeling and simulation is a powerful tool to improve and optimize the designs of the products. This paper presents a model and simulation results for the problem of self-heating unit of four food trays for group meals. Fig. 1 presents a one-dimensional (1D) model of a UGR-E unit [11]. As shown in Fig. 1a, the x-axis direction is along the height of the stack of the tray sets, from bottom to top. The dimensions (thicknesses) and material properties of the components are given in Table 1. The total height of the domain is 210 mm.

In order to examine temperature distribution within the heated food, five representative points P1–P5 in each food tray are considered. Fig. 1b shows the locations of these points. Point P1 is at the bottom of the food body (in contact with the food tray). Point P5 is at the top of the food body (in contact with the lid). Point P3 is at the center of points P1 and P5. Point P2 is at the center of P1 and P3; and point P4 is at the center of P3 and P5. Therefore, these five points evenly divide the food depth into four equal parts. From the dimensions listed in Table 1, the total depth of the food body in a tray is 40 mm, thus the distance between two adjacent points of interest is 10 mm.

2. Mathematical model

The governing equations for heat conduction through the components of the four-food tray heating system shown in Fig. 1a can be expressed as

$$\text{Cardboard}: \ \rho_c c_{p,c}\frac{\partial T}{\partial t} = \nabla(k_c \nabla T) \tag{1}$$

$$\text{Heating tray}: \ \rho_{pe} c_{p,pe}\frac{\partial T}{\partial t} = \nabla(k_{pe} \nabla T) \tag{2}$$

$$\text{Heater}: \ \rho_h c_{p,h}\frac{\partial T}{\partial t} = \nabla(k_h \nabla T) + q \tag{3}$$

$$\text{Food tray}: \ \rho_{pp} c_{p,pp}\frac{\partial T}{\partial t} = \nabla(k_{pp} \nabla T) \tag{4}$$

$$\text{Food}: \ \rho_f c_{p,f}\frac{\partial T}{\partial t} = \nabla\left(k_f \nabla T\right) \tag{5}$$

$$\text{Lid}: \ \rho_l c_{p,l}\frac{\partial T}{\partial t} = \nabla(k_l \nabla T) \tag{6}$$

$$\text{Air}: \ \rho_a c_{p,a}\frac{\partial T}{\partial t} = \nabla(k_a \nabla T) \tag{7}$$

The boundary conditions can be written as

$$\text{On bottom}: \ \mathbf{n}\cdot(k_c \nabla T) = 0 \tag{8}$$

$$\text{On top}: \ -\mathbf{n}\cdot(k_c \nabla T) = h(T - T_{amb}) \tag{9}$$

The initial condition can be written as

$$T = T_{init} \tag{10}$$

The source term q in Eq. (3) represents the heat generation rate per unit volume generated by the heater once activated. The requirements on magnesium–iron heater module currently used in the UGR-E are listed in the specification sheet MIL-DTL-32235/1 [11]. Details on the ingredients and operation are described in the US Patent 5,611,329 [6]. The heat generation is based on the exothermic reaction of reactive magnesium and water, which can be expressed as

$$Mg + 2H_2O \rightarrow Mg(OH)_2 + H_2 + \{Heat\}$$

The military specifications MIL-R-44398 [10] and MIL-DTL-32235/1 [11] describe the performance/capacity test for single heater for small MRE heater and large UGR-E heater, respectively. In the performance test for a heater, a food pouch or polymeric food tray filled with water is put on top of the heater in a heating tray. After the activation water is added into the heating tray, and is covered by a lid. Temperature rise is then recorded. In order to model the heat generation from a heater, a thermodynamic approach is employed for the control volume including the heater and the test food pouch, bounded by the heating tray and the lid in

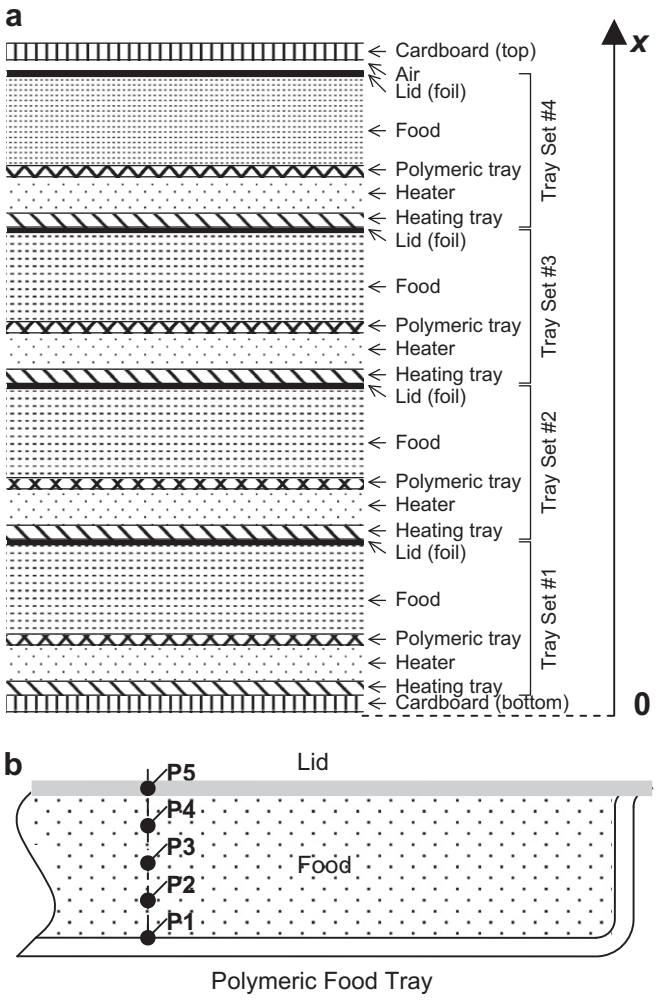

Fig. 1. Food self-heating system for group meals. (a) One-dimensional model; (b) representative points in a food tray.

the heater capacity test. For simplicity, it is assumed that there is no heat transfer through the boundary of the control volume. The governing equations of reaction and heat conduction for the control volume can be written as

$$\frac{d}{dt}m_r = -\lambda m_r \tag{11}$$

$$Q = \lambda m_r \Delta H_{rxn} \tag{12}$$

$$\left(m_h c_{p,h} + m_w c_{p,w}\right)\frac{dT}{dt} = Q \tag{13}$$

Table 1
Thickness and thermophysical properties of components.

Component (material)	Thickness	Density	Specific heat	Thermal conductivity
	δ, mm	ρ, kg/m^3	c_p, J/kg K	k, W/m K
Corrugated cardboard	4.1	145	1338	0.064
Heating tray (HDPE)	2.3	950	1900	0.5
Heater (Mg/saline)	6.3	1000	3284	171
Food tray (PP/…)	0.8	900	1800	0.2
Food (water/…)	40	1000	4180	0.6
Lid (Al/olefin/…)	0.2	2000	896	204
Air	3.4	1.16	1005	0.026

By solving Eqs. (11)–(13) with some proper simplifications, an approximate analytical solution for the temperature rise and heat generation rate can be found to have the forms

$$\Delta T = \Delta T_0[1 - \exp(-\lambda t)] \tag{14}$$

$$Q = Q_0 \exp(-\lambda t) \tag{15}$$

Total heat generation can be found as

$$G = \int_0^\infty Q dt = \frac{Q_0}{\lambda} \tag{16}$$

Assuming that the heat source is uniformly distributed over the entire space for the heater, the heat generation rate per unit volume can be found as

$$q = \frac{Q_0}{V_h}\exp(-\lambda t) \tag{17}$$

3. Numerical solution

The ambient and initial temperatures are taken as $T_{amb} = 23\ ^\circ C$, $T_{init} = 4\ ^\circ C$, which are consistent with testing conditions given in [11]. The dimensions in x-direction (thicknesses of layers in tray stack) and values of the physical properties of the materials in the system are listed in Table 1. The heat transfer coefficient on top of the domain is assigned a typical value for natural convection as $h = 10\ W/m^2\ K$

Lamensdorf [6] described a heater for use with an 8-ounce (226.8 g) MRE packet. The heater contains a mixture of 7.5 g magnesium 5 atomic weight percent iron super-corroding alloy and 1.5 g of nonreactive agents. The experimental data from the capacity test reported in [6] were reproduced as shown in Fig. 2. The curve fitting using the form in Eq. (14) yields

$$\Delta T = 71.85[1 - \exp(-0.002913t)] \tag{18}$$

From Eq. (18), the heat generation rate from the MRE heater can be found as

$$Q = 227.2\exp(-0.002913t) \tag{19}$$

Using Eq. (19), the heat generation of the heater can be calculated from Eq. (16) as 78 kJ. The results then can be extended to the larger heater used for the group meals heating unit UGR-E based on the fact that heat generation is proportional to the mass of the

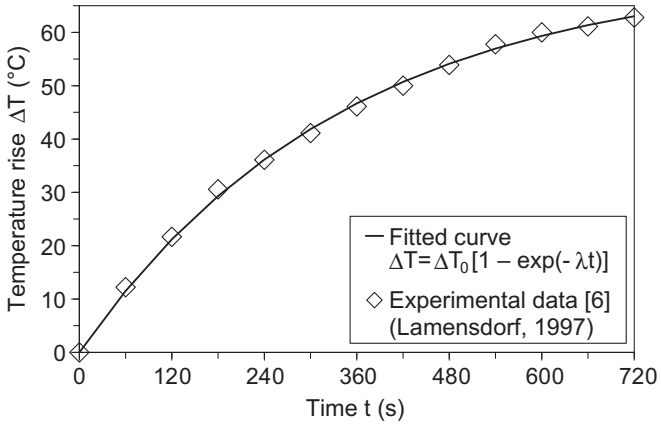

Fig. 2. Curve fitting of experimental data of temperature rise as function of time.

reactive agent. A heater that contains 60 g of reactive magnesium (8 times compared to that of the MRE heater) is considered. The heat generation of this heater can be calculated as 624 kJ. From Eqs. (15)–(17), the heat generation rate per unit volume of each UGR-E heater can be found as

$$q = 4 \times 10^6 \exp(-0.002913t) \quad (20)$$

Equation (20) can be plotted as shown in Fig. 3a. From Eq. (16), the heat generation G is obviously proportional to the area under this curve.

To solve the heat conduction problem using the finite element method, the computational domain needs to be discretized into a grid or mesh of small elements. For better accuracy, the mesh needs to have finer size elements (or higher mesh density) next to the boundaries where there are high temperature gradients. The temperature in each element was approximated by using the finite element method, which led to a set of nonlinear algebraic equations that defined the discretized continuum. This system of equations was solved using the time-dependent solver. The convergence criterion of absolute errors of the solutions was used with a tolerance set at 0.001 °C. The software COMSOL [13] was used to implement the numerical solution.

4. Results and discussion

Fig. 3 presents the results for the base case where all four heaters are identical and capable of generating heat of $G_b = 624$ kJ with a decay factor of $\lambda_b = 0.002913\ s^{-1}$. Fig. 3a shows the heating profile or the heat generation rate per unit volume in the form of an exponential decay function as formulated by Eq. (20). Fig. 3b presents the distribution of temperature over the entire computational domain at selected times of 1, 10, 20, 30, and 45 min. It can be observed that temperature distribution within each heater is almost uniform whereas it changes significantly within the food body of the four trays. The temperature profile at early times ($t = 1$ min, 10 min, etc.) shows four peaks which are corresponding to the locations of the heaters. This is the result of the exponential decay heating profile (Fig. 3) with high heat generation rate at early time. At $t = 45$ min, the temperature profile is smoothed out with a high temperature at the bottom and low temperature at the top of the stack of trays.

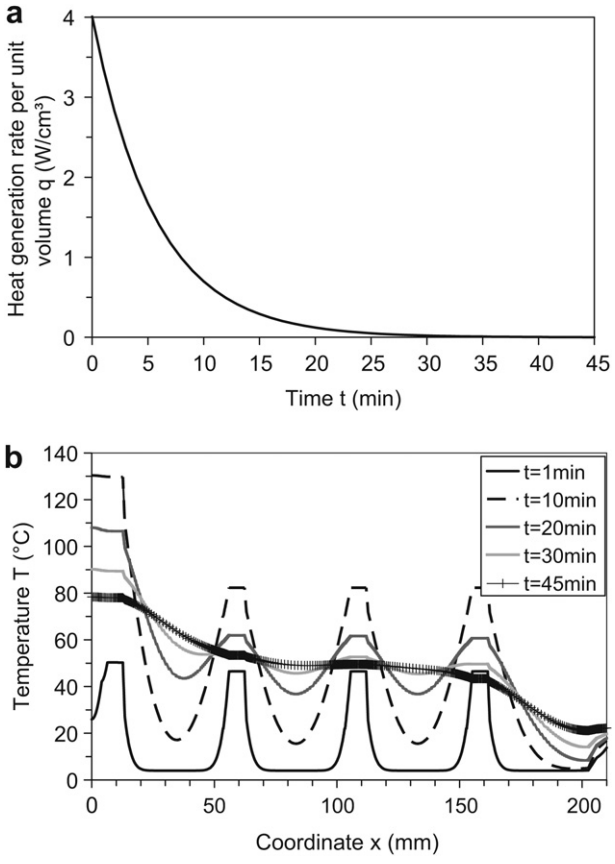

Fig. 3. Base case problem (a) heat generation rate per unit volume as function of time; (b) distribution of temperature at selected times.

Fig. 4 presents the food temperature as function of time in the four food trays. In each food tray, food temperature reaches its maximum value at the bottom of the food body (point P1), since this point is the closest to the heat source, at about 5–10 min after heater activation. Among the four food trays, tray 1 has the highest maximum temperature since it receives most of the heat generated by a heater because of the thermally insulated boundary condition at the bottom of the system. In Fig. 4a, it can be observed that temperature at P1 increases steeply from an initial value of 4 °C to a maximum value within $t = 10$ min then decreases gradually from that to about 30 °C lower at $t = 45$ min. Temperature at P5 follows the same trend with a peak of 40 °C lower than that of P1. Although having high temperature at first, P5 has the lowest temperature within the food body after 32 min. While P1 is under the influence of the heater right beneath it, P5 is affected mostly by the heater on top of it, which belongs to the next tray set. This heater supplies heat for both food tray 1 and 2 from top and from bottom, respectively. Temperature at points P2, P3, and P4 in tray 1 increases gradually as the result of heat conduction through the food medium from the higher temperature zones at the heaters. At $t = 45$ min, food temperature varies in a range of 20 °C within tray 1.

Fig. 4b and c show that the thermal behavior within trays 2 and 3 are symmetric and very similar to each other. Both trays are supplied by heat generation from two heaters on the top and bottom of the respective tray. For both trays, P1 and P5 have very close temperature curves that increase steeply to a peak at $t = 7$ min, then decrease gradually to a value of 20 °C lower than the peak at $t = 45$ min. Temperature curves of P2 and P4 are almost identical and increases slowly to a quasi-steady value at $t = 45$ min. At $t = 45$ min, food temperature varies in a range of about 5 °C within both trays 2 and 3.

Fig. 4d shows the thermal behavior of tray 4, which is on top of the stack of the heating unit. Temperature at P1 has the same curve as the other trays whereas temperature at P5 has no peak because there is no heater on top of it. Temperature variation at $t = 45$ min is about 20 °C.

As observed previously, temperature distribution in the two middle trays 2 and 3 look very similar. In order to quantify this similarity, food temperature difference between food trays 2 and 3 (denoted as F2 and F3) at the same location within each food tray (P1–P5) is plotted as functions of time as shown in Fig. 5. It shows that, for the first 10 min, temperature difference at all five points are almost zero. After that, they all increase monotonically at different slopes. It means that food temperature at a location in tray 2 is always higher than that in tray 3. Temperature difference at P5 has the highest increasing rate and highest value that reaches about 5 °C at $t = 45$ min. At P1, temperature difference has the same trend at second lower slope and reaches about 3.3 °C at $t = 45$ min. Lowest temperature difference is found at P3, which is at the center of the food.

From the arrangement of the heating system shown in Fig. 1, it can be expected that P1 mostly receives heat from the heater under it whereas P5 mostly receives heat from the heater above it,

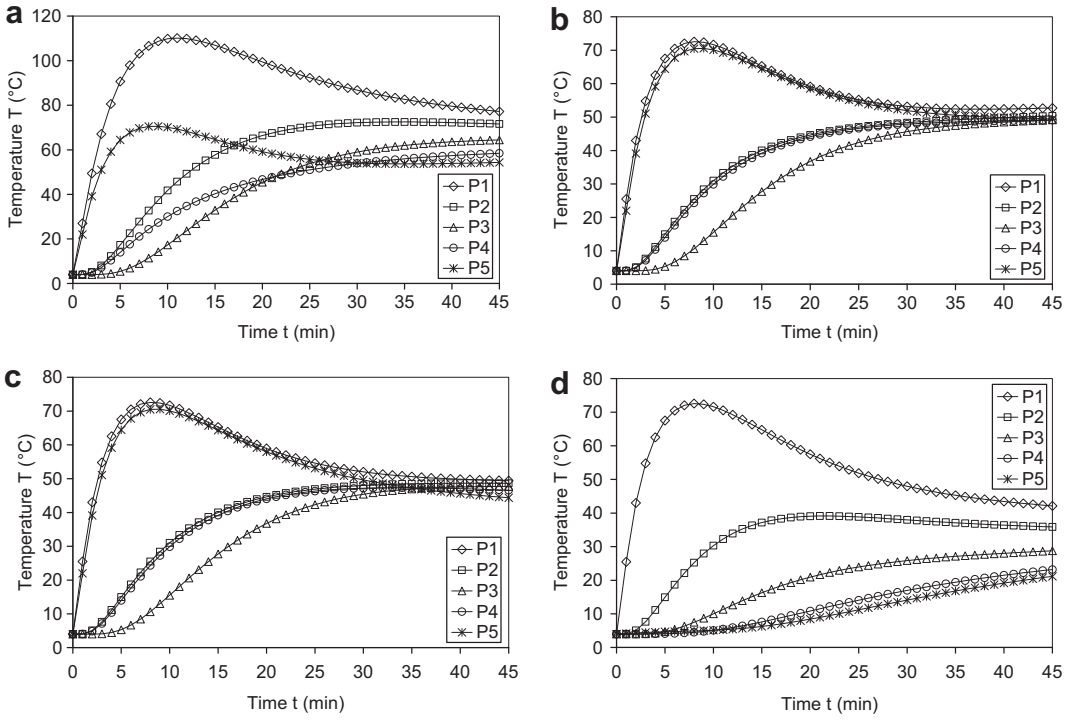

Fig. 4. Temperature as function of time at selected points in food trays: (a) tray 1 (bottom of stack); (b) tray 2; (c) tray 3; (d) tray 4 (top of stack).

which belongs to the next tray set. Different thicknesses and thermal conductivities affect the thermal resistance between the heat source and the points of interest, P1 and P5 on two side of a heater, therefore, cause different temperature response at these points. For P1 heat conducts through a thin wall of food tray from the beneath heater whereas for P5 through a three-time thicker wall of heating tray (and a thin lid) from the above heater. Fig. 6 shows the temperature difference between P5 of the beneath tray and P1 of the above tray for the three heaters 2, 3, and 4. It can be seen that for each pair of points of interest, for some early time the beneath P5 temperature is lower than the above P1 temperature up to 4 °C difference, then the former increases and exceeds the latter after 20, 40, and 17 min for heater 2, 3, and 4, respectively. At $t = 45$ min, temperature difference are 2.2, 1.6, and 0.1 °C, respectively. The curve corresponding to heater 3, which is between tray sets 2 and 3, and at the center of the stack, shows that the beneath P5 and the above P1 have almost the same temperature after about 30 min.

For the convenience in the following discussion, dimensionless decay constant λ^* and dimensionless heat generation G^* are defined as

$$\lambda^* = \frac{\lambda}{\lambda_b} \tag{21}$$

$$G^* = \frac{G}{G_b} \tag{22}$$

where $\lambda_b = 0.002913\ s^{-1}$ and $G_b = 624$ kJ are the base case values.

In order to study the effects of the rate of decay of the exponential decay heat source, several heating profiles that yield the same heat generation at different decay constants are considered. Fig. 7a shows four considered heating profiles under study. While having different decay constants of $\lambda^* = 1$, 2, 0.75, and 0.5, they all yield the same heat generation of $G^* = 1$. It can be observed that higher decay constant results in higher initial heat generation rate

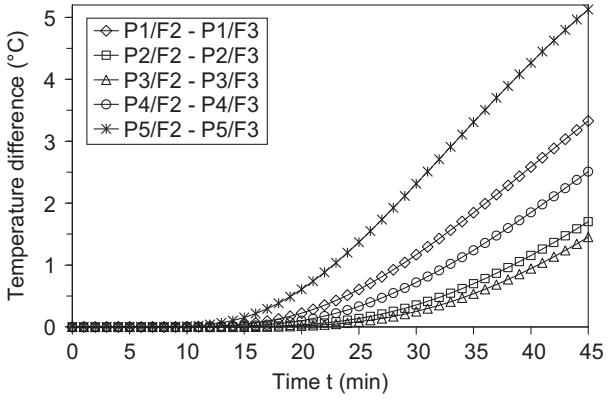

Fig. 5. Comparison of temperature distribution in food trays 2 and 3.

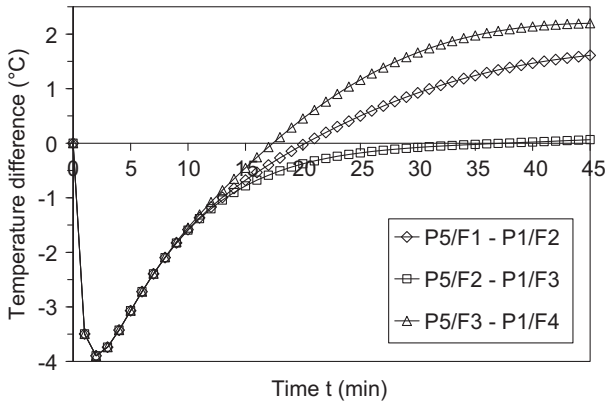

Fig. 6. Comparison of food temperature at closest points to heaters.

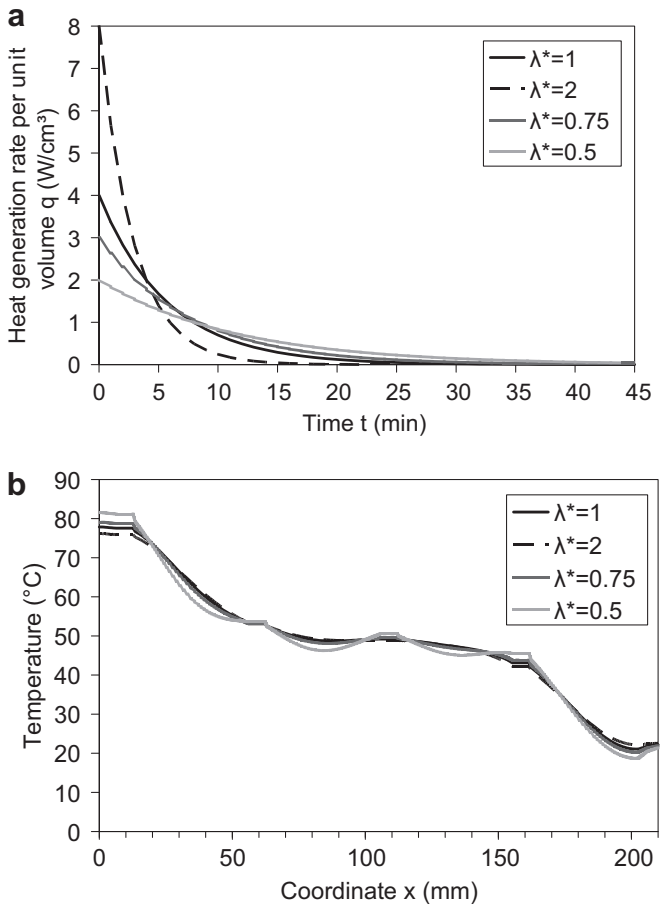

Fig. 7. Effects of decay constant. (a) heating profiles; (b) temperature distribution at $t = 45$ min.

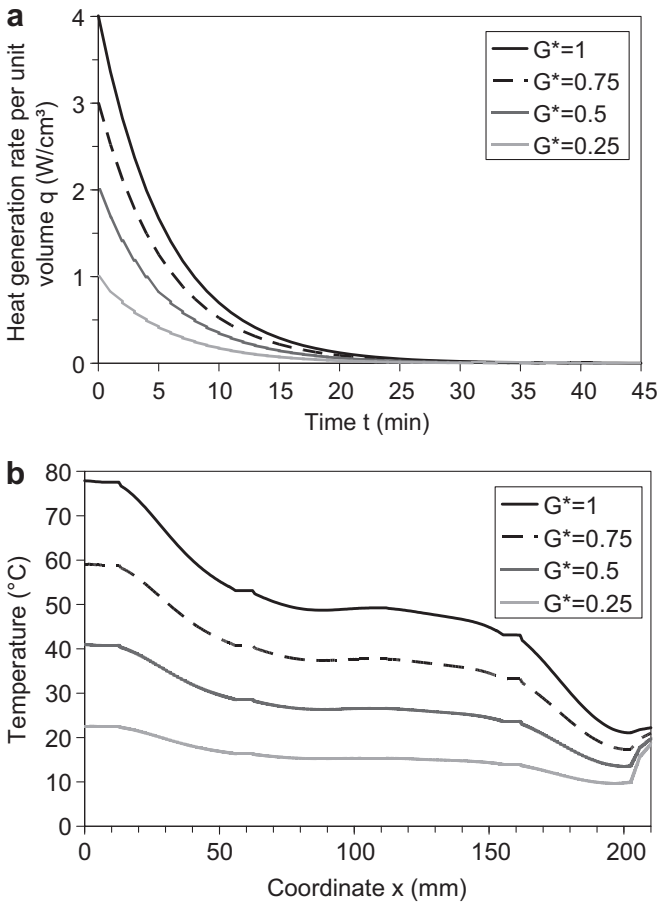

Fig. 8. Effects of heat generation. (a) heating profiles; (b) temperature distribution at $t = 45$ min.

and steeper initial decreasing rate. For each simulation case, four identical heaters having the same heating profiles are used. Fig. 7b presents the temperature distribution over the entire domain at $t = 45$ min for four simulation cases. It can be observed that the temperature distribution does not change significantly for $\lambda^* = 0.75$, 1, and 2. It can be expected that fast release heater, i.e., high decay constants have no significant effect on the temperature profile at $t = 45$ min. However, for λ^* as low as 0.5, temperature distribution in food trays 2 and 3 are no longer as uniform as in the base case with significantly lower temperature at the center of the food tray.

Fig. 8a shows the heating profiles with the same decay constant but generate different heat, represented by $G^* = 1$, 0.75, 0.5, and 0.25. The heating profile with lower G^* has lower initial heat generation rate but the same trend of exponential decay. For each simulation case, four identical heaters having the same heating profiles are considered. Temperature distribution at $t = 45$ min is shown in Fig. 8b. As it can be well expected, lower G^* (lower heat generation per heater) results in lower temperature over the entire domain while the trend remains the same.

From the observation above, it can be recognized that if all four heaters in the system are identical, temperature distribution at $t = 45$ min will always be different from food tray to food tray, despite the decay constant or heat generation per heater. One significant difference is that in food tray 1 (bottom tray) temperature is much higher and less uniform compared to that of tray 2 and 3. It is caused by the use of one heater at the bottom of the stack to supply heat to only one food tray 1, whereas each other heater has to supply heat to two food trays on both its sides. This suggests that the change in heat generation of the bottom heater can improve the thermal behavior of the system. Fig. 9 shows the effects of the changing heat generation in the bottom heater. This heat generation is represented by $G_1{}^*$, which is the ratio of heat generation in this heater to the reference value of that for the base case (624 kJ). It can be observed that the change of $G_1{}^*$ only affects temperature profile of tray 1 and slightly affects tray 2. As $G_1{}^*$ decreases, the temperature at the bottom of the stack decreases; and by that,

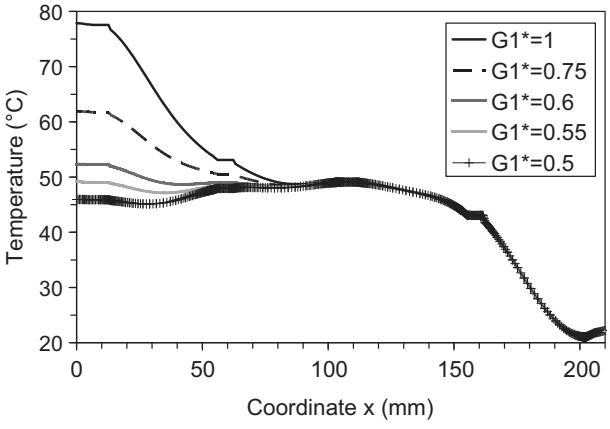

Fig. 9. Effects of heat generation in the first heater (at bottom of stack).

yields better temperature uniformity within tray 1. It is found that at $G_1^* = 0.55$, reasonable temperature uniformity is achieved with temperature variation within tray 1 of about 2 °C. This observation has a significant meaning since it provides a way of saving energy material and weight of heater, while maintaining adequate heating power and improving temperature uniformity in the multi-tray food-heating unit.

5. Conclusions

The numerical simulations provide insight to heat transfer in reactive and nonreactive systems and are instrumental for design of the food self-heating system. The results show that the food temperature at locations close to the heaters (bottom of all trays, top of trays 1, 2, and 3) rapidly increases from initial temperature to a peak temperature within 5–10 min after heater activation, then gradually decreases from there on down to 20–30 °C lower than respective peak temperatures at time of 45 min. During this time, food temperature at locations inside the food body increases gradually. At 45 min after heater activation, the temperature difference within food tray 1 (bottom) and 4 (top) is about 20 °C, whereas it is about 5 °C for trays 2 and 3.

It is expected from a food-heating unit that after a heating period, e.g., 45 min, (i) the food temperature is above a desired temperature, and (ii) the food temperature is uniformly distributed within the food body. The first criterion can be satisfied by utilizing heaters of high enough heat generation. For food temperature uniformity, the decay constant λ needs to be not too low, e.g., not less than about 0.002 s^{-1} for the system under study. The use of heater of lower heat generation for the bottom tray can improve the temperature difference between the bottom tray 1 and the middle trays 2 and 3. A combination of heaters with $G^* = 0.55$, 1, 1, 1, respectively, for trays 1, 2, 3, and 4 in the system under study yields a food temperature of 45–50 °C in trays 1–3. Since food temperature in the top tray 4 is dependent on the ambient temperature on its top and on one heater on its bottom, it is difficult to control the temperature uniformity there.

Acknowledgements

The authors would like to thank TempTroll LLC, Tampa, Florida, and Florida High Tech Corridor Matching Grant Program for financially supporting this research project.

References

[1] W.A. Caldwell, J. Gillies, Development of self-heating food can. Industrial Chemist 26 (306) (1950) 301–304.
[2] Anon, Progress of self-heating can in UK, Tin (1960) 141–142.
[3] M.T. Oliver-Hoyo, G. Pinto, J.A. Llorens-Molina, The chemistry of self-heating food products—an activity for classroom engagement. Journal of Chemical Education 86 (11) (2009) 1277.
[4] K.W. Kolb, U.S. Patent 7,004,161: Insertable Thermotic Module for Self-heating Cans. United States Patent and Trademark Office, 2006.
[5] D.W. Pickard, R.L. Trottier, P.G. Lavigne, U.S. Patent 5,355,869: Self-heating Group Meal Assembly and Method of Using Same. United States Patent and Trademark Office, 1994.
[6] M. Lamensdorf, U.S. Patent 5,611,329: Flameless Heater and Method of Making Same. United States Patent and Trademark Office, 1997.
[7] MIL-DTL-32235: Military Specification for Heater Module. Defense Logistics Agency, 2007, Available from: <www.dscp.dla.mil/subs/support/specs/mil/32235.asp>.
[8] M. Cox, Feed hot food to 18 soldiers fast. Army News (Oct. 30, 2006) Available from: <www.armytimes.com/legacy/new/1-292925-2320362.php>.
[9] What's Hot at Natick Soldier RD&E Center—Combat Feeding: Coming to a Theater Near You. Natick Soldier Research, Development and Engineering Center (NSRDEC), 2008, Available from: <nsc.natick.army.mil/hot/content.htm>.
[10] MIL-R-44398: Military Specification: Ration Supplement, Flameless Heater, for Meal, Ready-to-Eat. Defense Logistics Agency, 2003, Available from: <www.dscp.dla.mil/subs/support/specs/mil/44398.asp>.
[11] MIL-DTL-32235/1: Detail Specification Sheet—Heater Module, Type I: Magnesium and Iron Heater. Defense Logistics Agency, 2007, Available from: <www.dscp.dla.mil/subs/support/specs/mil/32235.asp>.
[12] UGR-E-001: unitized group ration express, Defense Logistics Agency, Available from: <www.dscp.dla.mil/subs/support/specs/pcrs/ugr/ugre.asp>.
[13] COMSOL AB, COMSOL Multiphysics software, version 3.4, Available from: <http://www.comsol.com/>.